

REMOTE SENSING OF TEMPERATURE PROFILES IN THE BOUNDARY LAYER

Liu Changsheng (刘长盛)

Department of Atmospheric Sciences, Nanjing University, Nanjing

Received November 15, 1986

ABSTRACT

The technique using a ground-based infrared broad-band scanning radiometer to measure temperature profiles in the boundary layer is suggested. The methods for retrieving and reducing its errors are discussed, and that of correction to water vapour absorption is also given.

I. INTRODUCTION

The remote sensing of temperature profiles by use of several narrow intervals in the 15 μm band of carbon dioxide from satellites has been used as the routine measurements for many years. Most of ground-based remote sensing of the temperature profiles have been done in the 5 mm microwave band of oxygen. Only a few works have been done in the infrared region. Wang et al. (1975) used a grating spectrometer to measure the downward flux of atmospheric radiance in twelve channels, eight in 15 μm carbon dioxide to retrieve the temperature profiles below 6 km, three in the 18 μm water vapour band to correct the water vapour absorption and one in the 11 μm window to detect clouds. Miyauchi and Kano (1981) did the similar work. Here we propose a different infrared ground-based sounding system, i.e. a broad-band and angle scanning system, to measure the temperature profiles in the boundary layer. The use of the broad-band has some advantages, e.g. the detectors with a lower detectivity can be used, the instrument is cheaper and easier to manufacture. Because of the very strong absorption in the 15 μm carbon dioxide band, the maximum detectable height of the atmospheric layer is limited. As a result of the angle scanning method, the spatial resolution is high. Therefore, it is very useful in measuring the temperature profiles in the boundary layer.

II. THE BAND AND MEAN ATMOSPHERIC TRANSMITTANCE

The instrument is a kind of filter scanning radiometer. Its detector is a bolometer. The transmittance of the filter is shown in Fig. 1. The mean transmittance over the band is

$$\bar{\tau} = \frac{\sum_{\nu=\nu_1}^{\nu_2} \tau_{\nu} F(\nu) \Delta\nu}{\sum_{\nu=\nu_1}^{\nu_2} F(\nu) \Delta\nu}, \quad (1)$$

where τ_{ν} is the atmospheric transmittance and $F(\nu)$ is the spectral response of the instrument.

The atmospheric model used in the calculations is listed in Table 1. The τ_p is calculated by the LOWTRAN 5 code and the mean transmittance for the model atmosphere is shown in Table 2.

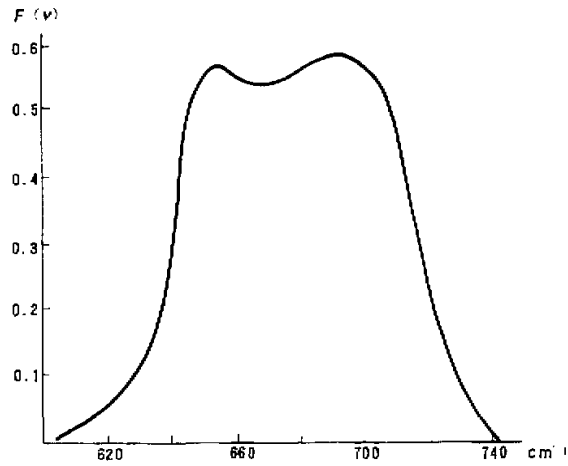


Fig. 1. Spectral response of the filter.

Table 1. Temperature and Humidity Profiles Used in the Calculation

H (m)	0	50	150	250	350	450	550	650	750
P (hPa)	10.3	1008	996	984	974	963	952	941	930
T (°C)	295.5	294.5	292.5	290.5	288.5	287.0	286.0	285.0	284.0
q_s (g/kg)	16.70	15.82	14.14	12.62	11.24	10.32	9.78	9.27	8.78

Table 2. Mean Transmittance in the Band

Thickness of layer (m)	50	150	250	350	450	550	650	750
$\bar{\tau}$	0.3696	0.1862	0.1217	0.08867	0.06910	0.05883	0.04660	0.03966

When the zenith angle increases, the slant path increases and the corresponding transmittance decreases. As the slant path increases to a certain length, the atmospheric layer becomes opaque. Table 3 lists the zenith angles for the different atmospheric layer at which the slant transmittance is less than 0.05. It shows that when the zenith angle is 78°, the first 50 m thickness from the surface layer upward appears blackened. If we measure the radiance at this angle, only the first 50 m atmospheric layer can be sensed. When the zenith angle is 65°, only the first 150 m atmospheric layer can be sensed, etc.

Table 3. Mean Transmittance for Slant Path

Thickness of layer (m)	50	150	250	350	450	550	650	750
Zenith angle	78	65	55	45	36	27	13	0
$\bar{\tau}$	0.04016	0.04354	0.04390	0.04551	0.04521	0.04360	0.04411	0.03966

III. TEMPERATURE RETRIEVING

If we measure the radiance at different zenith angles, listed in Table 3, the radiative transfer equation in these directions can be written as

$$\left. \begin{aligned} G_1 &= \sum_{\nu} B_{\nu}(T_1) \Delta\tau_{\nu}(z_1, L_1) F(\nu) \Delta\nu, \\ G_2 &= \sum_{\nu} B_{\nu}(T_1) \Delta\tau_{\nu}(z_2, L_1) F(\nu) \Delta\nu + \sum_{\nu} B_{\nu}(T_2) \Delta\tau_{\nu}(z_2, L_2) F(\nu) \Delta\nu, \\ &\vdots \end{aligned} \right\} \quad (2)$$

where z_i is the zenith angle, T_i is the mean temperature of the atmospheric layer, $L_i = 0-50$ m, $50-150$ m, $150-250$ m, ..., $650-750$ m, and $\Delta\tau_{\nu}(z_i, L_i)$ is the weighting function. The radiative transfer equation written as Eq. (2) means that the layer is treated to be blackened when the absorptivity of a layer is greater than 0.95. In Eq. (2) exist some truncated errors, which can be reduced if we select larger critical absorptivity or take the measurements at the corresponding greater zenith angles. Simultaneous Eq. (2) can be solved by stepwise iteration to get the temperature of each layer. Eq. (2) may be written in the matrix form

$$Af = G, \quad (3)$$

where A is the coefficient matrix with elements

$$A_{ij} = \frac{\sum_{\nu} B_{\nu}(T_j) \Delta\tau_{\nu}(z_i, L_j) F(\nu) \Delta\nu}{\sum_{\nu} B_{\nu}(T_j) F(\nu) \Delta\nu},$$

and

$$f_j = \sum_{\nu} B_{\nu}(T_j) F(\nu) \Delta\nu.$$

A_{ij} has the following approximate form

$$A_{ij} \approx \frac{\sum_{\nu} \Delta\tau_{\nu}(z_i, L_j) F(\nu) \Delta\nu}{\sum_{\nu} F(\nu) \Delta\nu},$$

which enable the weighting function to produce 1-2% errors, fortunately it just compensates some truncated errors. As a whole, this approximation will not cause serious errors.

In order to convert the radiance to the temperature, we calculate the radiance

$$R(\text{in } W\text{cm}^{-2}) = \sum_{\nu} B_{\nu}(T) F(\nu) \Delta\nu \quad (4)$$

in a proper temperature interval in advance. The relation between temperature T and radiance

R can be fitted by the Chebyshev polynomial as

$$T = 4.88826 \times 10^{10} R^3 - 1.3443363 \times 10^8 R^2 + 2.483346 \times 10^5 R + 176.2. \quad (5)$$

As a consequence, if Eq. (2) can be solved, the temperature profile will be retrieved. In fact, as mentioned above, Eq. (2) has included some truncated errors, and some measurement errors will be involved in the case of measurements, thus the retrieval will be unstable. Some constraints are needed in solving Eq. (2), which will be discussed in the following paragraphs.

IV. TEMPERATURE RETRIEVAL WHEN ERRORS EXIST

When the errors are included, Eq. (3) should be written as

$$Af = G + \epsilon = G', \quad (6)$$

The solution of Eq. (6), when the second finite differences is minimized, is

$$f' = (A^T A + \eta H)^{-1} A^T G, \quad (7)$$

where η is the smooth factor, and

$$H = \begin{pmatrix} 1 & -2 & 1 & & & & & & \\ -2 & 5 & 4 & 1 & & & & & \\ 1 & -4 & 6 & -4 & 1 & & & & \\ & & & & \ddots & & & & \\ & & & & & 1 & -2 & 1 & \end{pmatrix}$$

We did the numerical calculations according to Eq. (7). By choosing eight observational angles as shown in Table 3, eight radiances were calculated based on the radiative transfer equation for the atmosphere shown in Table 1. The retrievals in the case of adding random errors which are not more than 0.5 K equivalent radiation energy to the "measured radiance" are shown in Table 4, which gives the average values and the standard deviations of ten retrievals. It shows that the average retrieval is very close to the true profile, the standard deviation increases as the height increases. It also shows that when using greater smooth factors the retrieval results at higher layers will be improved. In fact, in the ground-based measurements it is not difficult to take several measurements at very short time. For example, it will be less than half a minute to take ten measurements by scanning radiometer. The use of the averaged value of measurements to do the retrieval will reduce random errors considerably.

Table 4. Retrieved Temperatures and Standard Deviations (averaged for ten measurements)

Layer	0-50	50-150	150-250	250-350	350-450	450-550	550-650	650-750
T (K)	295.0	293.5	291.5	289.5	287.8	286.5	285.5	284.5
0.02	295.1 ± 0.2	293.4 ± 0.3	291.6 ± 0.6	289.8 ± 1.2	288.1 ± 2.1	286.6 ± 3.2	285.0 ± 4.5	283.4 ± 5.9
0.05	295.0 ± 0.2	293.4 ± 0.5	291.6 ± 0.9	289.8 ± 1.1	287.9 ± 1.6	286.1 ± 2.2	284.3 ± 3.1	282.5 ± 4.0
η 0.10	295.0 ± 0.1	293.5 ± 0.2	291.9 ± 0.5	290.4 ± 0.8	288.8 ± 1.2	287.3 ± 1.6	285.7 ± 2.1	284.1 ± 2.7
0.50	295.0 ± 0.2	293.5 ± 0.2	292.0 ± 0.5	290.5 ± 0.9	288.9 ± 1.2	287.4 ± 1.1	285.8 ± 2.0	284.2 ± 2.3

V. RETRIEVALS UNDER THE BOUNDARY LAYER INVERSION

The accuracy of retrievals depends upon that of the weighting function. We did some numerical experiments to see how the results are affected by the weighting function. Table 5 gives an example of the boundary layer inversion, Table 6 the corresponding mean transmittance for different thicknesses of atmosphere at different zenith angles, and Table 7 the retrieval results for different weighting functions. It is shown from Table 7 that both T_2 and T_3 do give the inversion but much stronger than the real one. If we have the correct weighting func-

tion, we can do the retrieval more accurately even in the situation of inversion. Fortunately, some useful information can be acquired from the measurements. The variation of the radiance with zenith angles is quite different during inversion from that in normal temperature distributions. Fig. 2 shows that during normal temperature distributions the radiance increases with increasing zenith angles, but if an inversion exists the radiance will decrease with increasing zenith angles. Thus, glancing at the variation of the radiance with zenith angles will know the temperature profile cursorily. That will help us to choose the correct weighting function.

Table 5. Boundary Layer Inversion

H (m)	0	50	150	250	350	450	550	650	750
P (hPa)	1024	1018	1006	994	982	970	958	946	934
T (C)	275.8	277.1	279.0	279.6	279.1	278.6	278.2	277.5	276.8
q _s (g/kg)	4.54	5.00	5.78	6.10	5.97	5.84	5.75	5.54	5.34

Table 6. Mean Temperature for Table 5

Thickness of Layer (m)	50	150	250	350	450	550	650	750
Zenith angle (deg)	87	80	74	66	58	49	39	29
\bar{T}	0.04405	0.04855	0.04558	0.04839	0.04948	0.05070	0.05144	0.05071

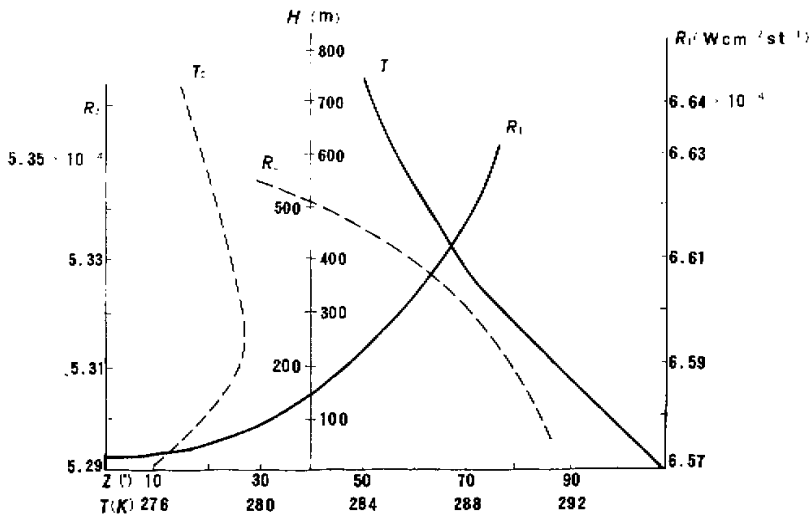


Fig. 2. The variation of radiance with zenith angle for different temperature profiles.

Table 7. Temperature Retrieval under Boundary Layer Inversion

Layer (m)	0-50	50-150	150-250	250-350	350-450	450-550	550-650	650-750
T	276.5	278.1	279.3	279.4	278.9	278.4	277.9	277.2
T_1	276.7	278.4	279.3	279.9	279.2	278.8	278.2	277.2
T_2	276.8	279.7	280.8	280.2	278.7	277.8	277.0	275.6
T_3	276.9	279.2	280.4	280.8	280.4	279.6	278.7	277.7

T_1 —Retrieved temperature using the correct weighting function ($\eta=0$)

T_2 —Retrieved temperature using the weighting function of isothermal atmosphere ($\eta=0$, $T=276.0$, $q_1=4.5$ g/kg)

T_3 —Retrieved temperature using the weighting function of isothermal atmosphere ($\eta=0.005$, $T=276.0$, $q_1=4.5$ g/kg)

VI. EFFECTS OF WATER VAPOUR ABSORPTION

Over the 15 μm carbon dioxide band there is water vapour absorption overlapped. This may influence the weighting function. The error in weighting function will be propagated into the retrieved temperature profile in the form of systematic error (Fleming et al., 1983). According to numerical calculations, as the specific humidity increases the weighting function will be reduced in the lower layer and increased in the upper layer. For example, in the atmosphere shown in Table 1, when the relative humidity increases from 60% to 100% the weighting func-

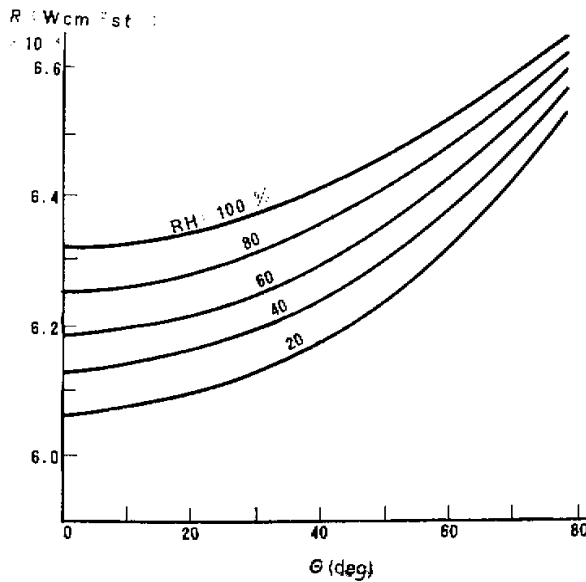


Fig. 3. The variation of the radiance with the zenith angles for the same temperature profile but with different relative humidity.

tion will be reduced by 4% at ground and increased by more than 10% at the top layer. But the mainly influenced layer is near the ground. Fig. 3 illustrates the variation of the radiance with the zenith angles for a temperature distribution shown in Table 1 but with different relative humidities. These five curves in Fig. 3 are all corresponding to the same temperature profile. This means that five sets of radiance may give the same retrieved temperature but have to use five different weighting functions. This is not convenient for the retrieving. Instead, we use one weighting function but with the radiance corrected to its corresponding humidity to do the retrieval. In this situation the humidity distribution is needed. Because the layer influenced by water vapour is near the ground, if we measure the humidity at the ground and assume the relative humidity to be constant, then the water vapour absorption can be corrected.

VII. CONCLUDING REMARKS

Based on the previous discussion we can draw the following conclusions:

- (1) It is feasible to retrieve the temperature profiles in the boundary layer by broad-band measurements at well-chosed different zenith angles in the 15 μm carbon dioxide band at the ground.
- (2) Retrieval errors can be minimized by using the averaged measurements which are taken within a very short time interval.
- (3) The variation of radiance with zenith angles can reveal the temperature profile that will help us to choose the optimal weighting function.
- (4) Water vapour influence can be corrected by using the ground truth and the assumption of relative humidity as a conservative factor.

REFERENCES

- Fleming, H.E., Crosby, D.S. and Neuendorffer, A.C. (1983), Elimination of a major error component in satellite temperature sounding, Fifth Conference on Atmospheric Radiation, Oct. 31-4 Nov., pp. 20-22.
- Miyauchi, M. and Kano, M. (1981), Influence of atmospheric temperature from measurements with the ground-based spectrometer, *Paper in Meteor. and Geophys.*, **32**:pp. 291-299.
- Wang, J.Y., Claysmith, C.R. and Griggs, M. (1975), Measurement of lower atmospheric temperature profiles from ground-based infrared observations, *J. Appl. Meteor.*, **14**:pp. 308-318.

